Redox Biology 19 (2018) 318–330

Contents lists available at ScienceDirect

Redox Biology

journal homepage: www.elsevier.com/locate/redox

Research paper

25-Hydroxycholesterol and 27-hydroxycholesterol inhibit human rotavirus infection by sequestering viral particles into late endosomes

Andrea Civra, Rachele Francese, Paola Gamba, Gabriella Testa, Valeria Cagno[1], Giuseppe Poli*, David Lembo*

Department of Clinical and Biological Sciences, University of Turin, Regione Gonzole 10, 10043 Orbassano, TO, Italy

A B S T R A C T

A novel innate immune strategy, involving specific cholesterol oxidation products as effectors, has begun to reveal connections between cholesterol metabolism and immune response against viral infections. Indeed, 25-hydroxycholesterol (25HC) and 27-hydroxycholesterol (27HC), physiologically produced by enzymatic oxidation of cholesterol, act as inhibitors of a wide spectrum of enveloped and non-enveloped human viruses. However, the mechanisms underlying their protective effects against non-enveloped viruses are almost completely unexplored. To get insight into this field, we investigated the antiviral activity of 25HC and 27HC against a non-enveloped virus causing acute gastroenteritis in children, the human rotavirus (HRV). We found that 25HC and 27HC block the infectivity of several HRV strains at 50% inhibitory concentrations in the low micromolar range in the absence of cell toxicity. Both molecules affect the final step of virus penetration into cells by preventing the association of two cellular proteins: the oxysterol binding protein (OSBP) and the vesicle-associated membrane protein-associated protein-A (VAP-A). By altering the activity of these cellular mediators, 25HC and 27HC disturb the recycling of cholesterol between the endoplasmic reticulum and the late endosomes which are exploited by HRV to penetrate into the cell. The substantial accumulation of cholesterol in the late endosomal compartment results in sequestering viral particles inside these vesicles thereby preventing cytoplasmic virus replication. These findings suggest that cholesterol oxidation products of enzymatic origin might be primary effectors of host restriction strategies to counteract HRV infection and point to redox active lipids involvement in viral infections as a research area of focus to better focus in order to identify novel antiviral agents targets.

Introduction

Innate immune response is the first line of defense during the earliest hours of exposure to a novel pathogen. Its mechanisms are non-specific and rely on a group of proteins and phagocytic cells that quickly activate to help destroy invaders. Alongside these pathways, a novel innate immune strategy has begun to reveal connections between cholesterol metabolism and immune response against viral infections. [1–3].

The most widely studied effector of this branch of innate immunity is an oxysterol, 25-hydroxycholesterol (25HC) [1,2]. Oxysterols contain 27 carbon atoms per molecule and are derived from cholesterol by both enzymatic and nonenzymatic oxidation [4–6]. Several among the various cholesterol oxidation products of enzymatic origin contribute to physiological functions: they are intermediates of pregnenolone and steroid hormone synthesis [7] and target nuclear receptors (e.g., the liver X receptor [LXR] and the estrogen receptor α [ER α]), cellular membrane receptors (e.g., C-X-C motif chemokine receptor 2 [CXCR2]) and transport proteins (e.g., insulin induced gene protein [INSIG], Niemann-Pick protein 1 [NPC1], oxysterol binding protein [OSBP] and its related proteins [ORPs]) [8–13]. In contrast, the oxysterols derived from cholesterol autoxidation, a not-regulated and therefore potentially harmful biochemical reaction, appear to be more likely involved in pathophysiological processes associated with inflammation and oxidative stress [4,5,14].

In 2013 Blanc and colleagues provided in vitro findings indicating that 25HC acts as a physiological interferon (IFN)-induced effector of innate immunity against viral infections [1]. They reported that 25HC was the only oxysterol synthesized and secreted by macrophages upon IFN treatment or virus infection and that transcription factor Stat1 directly couples IFN-stimulated signaling to regulation of the cholesterol hydroxylase gene (Ch25h) encoding the 25HC-synthesizing enzyme.

Unlike known antiviral small molecules that target highly specific viral determinants, thus showing a restricted spectrum of activity, 25HC inhibits the replication of a wide spectrum of pathogenic viruses. This includes both enveloped viruses, i.e., those with a phospholipidic bilayer outside the proteic capsid such as human immunodeficiency virus (HIV), herpes simplex virus type 1 (HSV-1), varicella zoster virus (VZV) murine cytomegalovirus (MCMV), vesicular stomatitis virus (VSV), Ebola virus (EBOV), Zika virus, hepatitis C virus, and

* Corresponding authors.
E-mail addresses: giuseppe.poli@unito.it (G. Poli), david.lembo@unito.it (D. Lembo).
[1] Present address: Valeria Cagno, Institute of Materials, Ecole Polytechnique Fédérale de Lausanne (EPFL), Lausanne, Switzerland.

https://doi.org/10.1016/j.redox.2018.09.003
Received 3 August 2018; Received in revised form 29 August 2018; Accepted 3 September 2018
Available online 05 September 2018

Table 1
Antirotavirus activity of oxysterols (MA104 cells).

Oxysterols	HRV strain	EC_{50}[a] (μM) – 95% CI[b]	EC_{90}[c] (μM) – 95% CI	CC_{50}[d](μM) –95% CI	SI[e]
25HC	Wa	0.16 (0.12–0.20)	1.37 (0.75–2.40)	> 150	> 938
	WI61	0.09 (0.08–0.12)	0.28 (0.16–0.46)	> 150	> 1667
	HRV408	0.12 (0.09–0.16)	0.42 (0.23–0.74)	> 150	> 1250
	HRV248	0.11 (0.07–0.18)	1.26 (0.47–3.38)	> 150	> 1364
	DS-1	0.27 (0.14–0.53)	5.77 (1.15–28.89)	> 150	> 556
27HC	Wa	0.26 (0.22–0.31)	1.73 (1.21–2.47)	> 150	> 577
	WI61	0.19 (0.14–0.27)	0.74 (0.35–1.55)	> 150	> 790
	HRV408	0.40 (0.26–0.62)	4.56(1.62–12.82)	> 150	> 375
	HRV248	0.23 (0.12–0.46)	3.84 (0.80–18.39)	> 150	> 652
	DS-1	0.72 (0.49–1.06)	5.85 (2.43–14.06)	> 150	> 208

n.a. not assessable.
[a] EC_{50} half-maximal effective concentration.
[b] CI confidence interval.
[c] EC_{90}90% effective concentration.
[d] CC_{50} half maximal cytotoxic concentration
[e] SI selectivity index.

orthomixovirus [1,2,15–19], and non-enveloped viruses such as human rhinovirus (HRhV) [20–22], human papillomavirus (HPV), and human rotavirus (HRV) [21].

This unprecedented range of antiviral properties is ascribable to the ability of 25HC to modulate cellular lipid metabolism and transport, thereby modifying the composition and structure of cellular and subcellular membranes [23,24]. Since viral pathogens have to pass through cellular lipid membranes or hijack them to assemble their replicative machinery, regulation of the lipid composition of cellular and subcellular membranes looks like a particularly smart and effective strategy to counteract viral invasion from a strictly evolutionary point of view.

The mechanisms underlying the antiviral activity of 25HC have been extensively investigated for a number of enveloped viruses: 25HC might alter the lipid composition of cellular membranes, thus hampering the fusion between the viral envelope and the cytoplasmic lipid bilayer that allows some enveloped viruses to penetrate into the host cell [1]. This oxysterol directly changes cell membrane properties by inserting itself into the lipid bilayer [2]. Moreover, various studies on 25HC-induced host response to HCV infection clearly correlated this protective action with an imbalance in the mevalonate pathway by the oxysterol [17,25–27], implying the inhibition of cholesterol synthesis and depletion of non-sterol isoprenoid products, in this way impairing cholesterol membrane content and protein prenylation [17,25–28]. Of note, our group showed that 25HC but also a second enzymatically synthesized oxysterol, 27-hydroxycholesterol (27HC) can stimulate the release of interleukin 6 (IL6) and are endowed with an anti-HSV-1 activity which is apparently non-unrelated to the viral entry inhibition [19].

By contrast, the mechanisms underlying the protective effects of cholesterol oxidation products against non-enveloped viruses are largely unexplored, with the unique exception of HRhV [22] and 25HC as the only oxysterol examined so far [22]. In fact, this oxysterol has been shown to markedly reduce the accumulation of phosphatidylinositol 4-phosphate (PI4P) in the Golgi apparatus, a crucial event for the assembly of HRhV replicative machinery, by targeting members of the OSBP family I [20,22].

With regard to non-enveloped viruses, we previously described the antiviral activity exerted by 25HC and 27HC, particularly against HRV [21]. We investigated the mechanism of action of 25HC and 27HC against HRV to shed a light on an almost totally unexplored scenario, which may hold promise to reveal novel antiviral mechanisms and targets, likely exploitable for a new generation of antiviral molecules.

HRV belongs to the reoviridae family and represents one of the leading causes of infective gastroenteritis in children [29]. Its genome consists of 11 segments of double-stranded RNA encoding six structural proteins (VP1–VP4,VP6, and VP7) and six non-structural proteins (NSP1–NSP6). The mature virion is a triple-layered particle (TLP) about 100 nm in diameter and consists of an inner layer (the core) composed of the viral proteins VP1 and VP2, an intermediate layer (the inner capsid made of VP6), and an outer layer (the outer capsid consisting of VP7 and projections of VP4) [30,31], with VP4 being the major determinant of tropism and receptor binding [32–35].

HRVs exploit the endocytic route to enter cells. Various human strains, such as HRV Wa, WI61, and DS-1, travel along this intracellular path to reach the late endosomes (LEs) [36]. Once inside the LEs, a sequence of molecular transformations in the outer-layer proteins VP7 and VP4 strips the proteins from the virion (i.e., the TLP) and delivers into the cytosol an inner capsid particle, known as the double-layered particle or DLP [37].

Here we report on an original mechanism of antiviral action by oxysterols against HRV. We found that both 25HC and 27HC block HRV cell entry and replication by inducing an accumulation of cholesterol in the LEs, thereby sequestering viral particles inside these vesicles. These findings represent a step forward in our understanding the role oxysterols play as effectors of innate immunity against viral infections.

Results

Anti-HRV effect of 25HC and 27HC and their spectrum of activity

In a previous study, we reported on the inhibitory activity of 25HC and 27HC against the Wa strain of HRV [21]. To explore the spectrum of anti-HRV activity, 25HC and 27HC were tested against four additional HRV strains (WI61, HRV 408, HRV 248, DS-1) in MA104 cells. As shown in Table 1, the antiviral activity of both 25HC and 27HC is not strain-restricted, with EC_{50} values falling in the low micromolar range and favorable selectivity index (SI) for all the HRV strains tested. Both oxysterols inhibited HRV infection in a dose-dependent fashion (Fig. 1). The antiviral potency of 25HC was significantly ($p_{Ftest} < 0.001$) higher than that of 27HC against each strain tested. Since most of the assays of the mechanism of action described below were performed by testing 25HC and 27HC against high viruses/target cell ratios (MOI, multiplicity of action), we verified that both molecules were able to inhibit HRV infectivity also under these conditions. Indeed, they significantly inhibited HRV infectivity to a maximum of 90% even at high MOI (MOI 10) (Fig. 3). Finally, 25HC and 27HC were also tested against HRV infection of human intestinal Caco2 cell line to determine whether their antiviral activity was influenced by the cellular model. The two oxysterols displayed a strong antiviral effect in both MA104 and Caco2 cells, two quite different cellular models (Tables 1 and 2; Figs. 1 and 2), thus indicating that their activity is not cell line dependent.

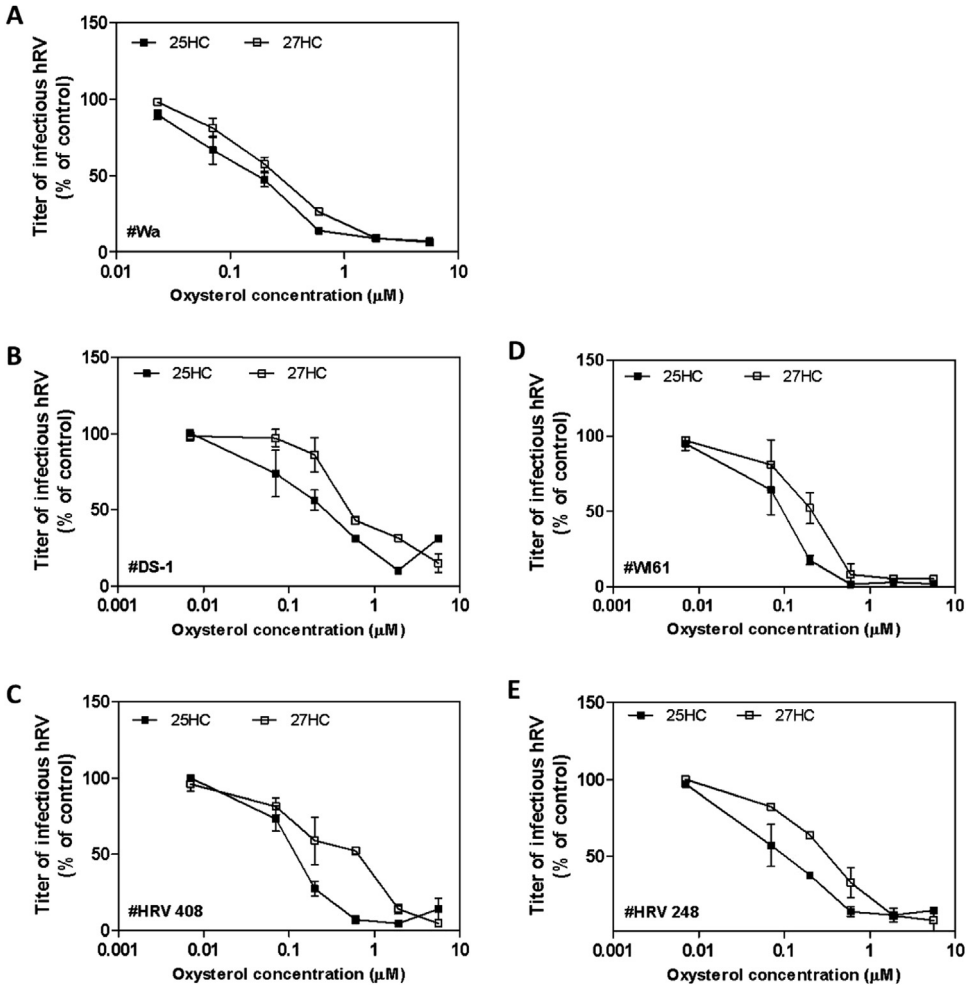

Fig. 1. Antiviral activity of 25HC and 27HC against HRV strains Wa (A), DS-1 (B), HRV 408 (C), WI61 (D), and HRV 248 (E) on MA104 cells. Cells were treated for 20 h with increasing concentrations of oxysterols and then infected. Viral infections were detected as described in the Material and Methods section. The percentage infection was calculated by comparing treated and untreated wells. The results are means and SEM for triplicates.

Table 2
Antirotavirus activity of oxysterols (Caco2 cells).

Oxysterols	HRV strain	EC_{50}[a] (μM) – 95% CI[b]	EC_{90}[c] (μM) – 95% CI	CC_{50}[d] (μM) –95% CI	SI[e]
25HC	Wa	0.19 (0.14–0.25)	1.26 (0.61–2.60)	> 150	> 789
	WI61	0.25(0.20–0.31)	0.83(0.50–1.38)	> 150	> 600
	HRV408	0.42(0.36–0.48)	2.30(1.66–3.18)	> 150	> 357
	HRV248	0.21(0.16–0.28)	1.04(0.55–1.94)	> 150	> 714
	DS-1	0.43 (0.29–0.63)	2.42 (1.04–5.63)	> 150	> 349
27HC	Wa	0.44 (0.34–0.56)	2.50 (1.45–4.29)	> 150	> 341
	WI61	0.34(0.22–0.53)	2.43(0.90–6.59)	> 150	> 441
	HRV408	0.81(0.60–1.09)	3.78(1.94–7.36)	> 150	> 185
	HRV248	0.41(0.35–0.48)	2.70(1.90–3.83)	> 150	> 366
	DS-1	0.45 (0.34–0.61)	2.62 (1.37–5.03)	> 150	> 333

n.a. not assessable.
[a] EC_{50} half-maximal effective concentration.
[b] CI confidence interval.
[c] EC_{90}90% effective concentration.
[d] CC_{50} half maximal cytotoxic concentration.
[e] SI selectivity index.

25HC and 27HC inhibit HRV-cell penetration

Specific assays were performed to identify which step(s) of the HRV replicative cycle was inhibited by the two oxysterols. Time-of-addition assays showed that 25HC and 27HC exerted their highest antiviral efficacy when added to cells 20 h before infection (Fig. 4A-B). By contrast, when the treatment was performed after viral infection, no antiviral effect was observed. These data suggest that both oxysterols modify the cellular milieu so as to render the cells less susceptible to HRV most likely by targeting cellular determinants essential for virus

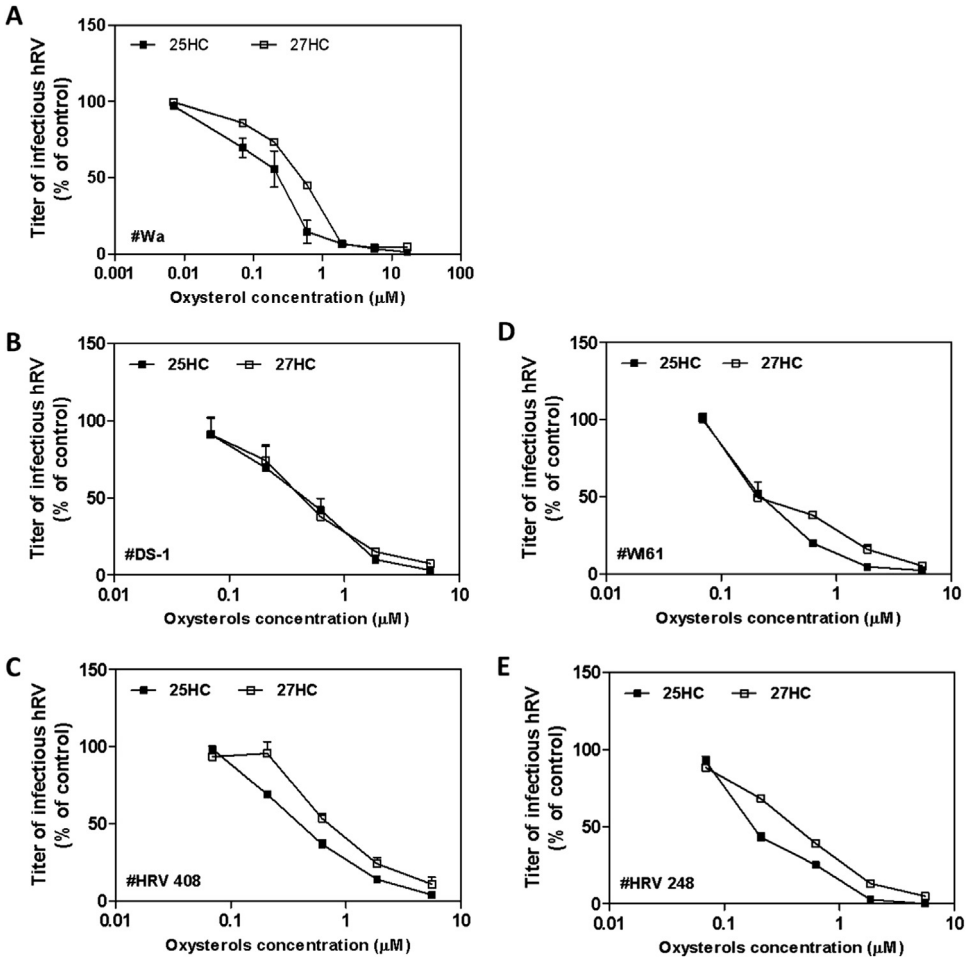

Fig. 2. Antiviral activity of 25HC and 27HC against HRV strains Wa (A), DS-1 (B), HRV 408 (C), WI61 (D), and HRV 248 (E) on Caco2 cells. The results are means and SEM for triplicates.

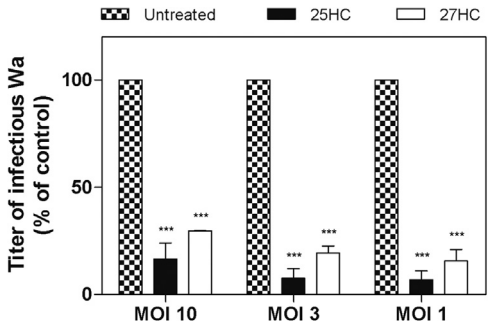

Fig. 3. Antiviral activity of 25HC and 27HC against HRV Wa at multiplicity of infection (MOI) 10, 3, and 1 on MA104 cells. Cells were treated for 20 h with 25HC or 27HC at EC90 concentrations and then infected. Viral infections were detected as described in the Material and Methods section. The percentage infection was calculated by comparing treated and untreated wells. The results are means and SEM for triplicates. ***$p_{ANOVA} < 0.001$.

penetration or replication. Of note, as displayed in Fig. 4C, the indirect immunocytochemistry clearly shows that no deposition of neo-synthetized HRV antigen occurs in both MA104 and Caco2 cells at 20 h post infection, when infection was stopped by fixing cells. Taken together, these results suggested that 25HC and 27HC were able to affect the steps of the HRV replicative cycle occurring before HRV protein synthesis. For this reason, we investigated the effect of oxysterols on the earliest steps of HRV replication, i.e. virus binding and penetration. Binding assay experiments clearly showed that treatment with both 25HC and 27HC had no effect on HRV attachment to the cell surface (Fig. 5 panel A).

In a second set of experiments, we assessed the ability of the oxysterols to alter HRV entry kinetics into the cells. Both 25HC and 27HC significantly ($0.001 < p_{ANOVA} < 0.05$) hampered normal virus-cell penetration, when measured as a function of viral particles that enter cells and carry out a single replication cycle (Fig. 5B). Consistent with previous results (Fig. 1), 25HC affected HRV entry kinetics more potently than 27HC.

HRV penetration into the host cell is a complex event involving receptor-mediated endocytosis, LE membrane permeabilization, and release of the virus particle into the cytoplasm where viral replication occurs. Interestingly, when we forced by means of Lipofectamine the infection of an ethylene glycol tetraacetic acid (EGTA)-inactivated HRV suspension, thereby bypassing viral entry through endocytosis, 25HC and 27HC showed no antiviral activity (Fig. 5C). Consistently with these results, when we added oxysterols on infected cells after NH_4Cl treatment (i.e. after the HRV exit from LEs) no antiviral activity was measurable (Fig. 5D). More importantly, we analyzed the intracellular localization of HRV 8 h post-inoculum, when most of the virus particles have already escaped from the LEs and replicate in the cytoplasm where newly synthesized viral proteins accumulate. As expected, confocal immune microscopy revealed that the viral antigen VP6 was mostly diffused in the cytoplasm of untreated infected cells (Fig. 6). By contrast, in both the 25HC- and the 27HC-treated cells, almost all VP6 co-localized with a marker of LEs (Rab-7). Taken together, these results indicate that 25HC and 27HC affect HRV entry by sequestering the virus particles penetrating the LEs and preventing their replication in the cytoplasm.

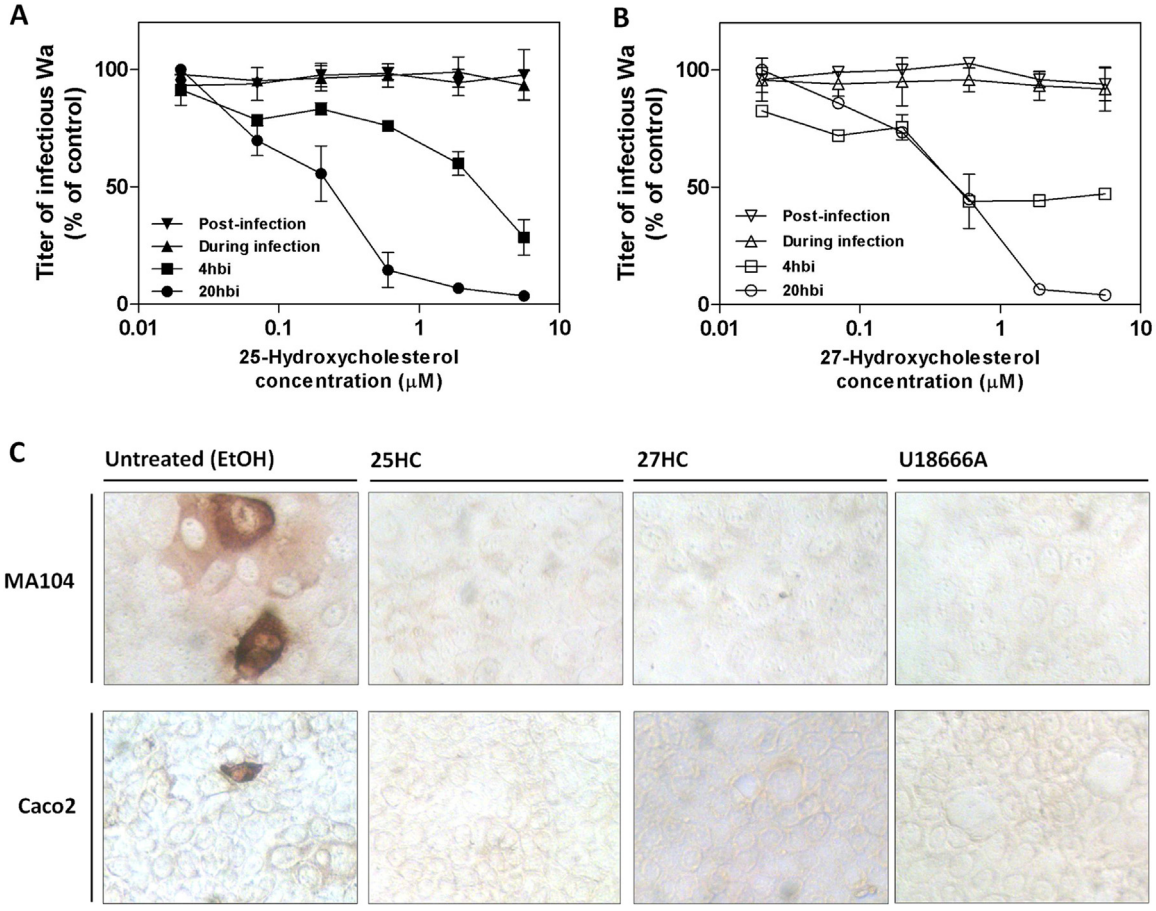

Fig. 4. Time of addition experiments. Panels A and B: time-of-addition experiments were performed by treating cells with 25HC(A) or 27HC(B) for 20 h or 4 h before infection, for 1 h during infection or by adding the oxysterols immediately after infection. The infectivity titers of virus in the treated samples are expressed as a percentage of the titer obtained in the absence of treatment. Error bars represent the standard error of the mean (SEM) of 3 independent experiments. Panel C shows the effect of oxysterols on deposition of neosynthetized VP6 antigen as assessed by immunocytochemistry. Infected MA104 or Caco2 cell lines were fixed at 20 h post-infection and stained with anti-VP6 antibody.

OSBP and VAP-A are cellular determinants of 25HC and 27HC anti-HRV activity

To elucidate the mechanism by which 25HC and 27HC block HRV penetration in the LEs, we focused our attention on the cellular protein OSBP, one of the main intracellular interactors of oxysterols. Proteins that prevent OSBP association with the vesicle-associated membrane protein-associated protein A (VAP-A) are known to disrupt intracellular cholesterol homeostasis, leading to cholesterol accumulation on the LEs membrane. This event has been shown to inhibit the entry of specific enveloped viruses [38,39]. Although this mechanism has been postulated only for enveloped viruses, we hypothesized that the model of a "greasy response" to viral infection - as defined by Tanner and colleagues in 2013 [39] - could fit with our results (Fig. 6). In specific assays to verify whether this mechanism applies to the anti-HRV activity of oxysterols, first we used co-immunoprecipation assays to assess whether physical interaction between OSBP and VAP-A was disrupted in 25HC- or 27HC-treated MA104 cells.

Immunoprecipitation of VAP-A co-immunoprecipitated OSBP in untreated cells and the reverse was demonstrated (Fig. 7A). Co-immuneprecipitation was specific since neither VAP-A nor OSBP was detected in the immunoprecipitates obtained with an unrelevant antibody used as a negative control. This result was consistent with previous studies that showed a physical interaction between OSBP and VAP-A. Interestingly, we found that the association of OSBP to VAP-A was disrupted in the 25HC- or 27HC-treated cells. Control experiments showed that the treatment did not down-regulate OSBP and VAP-A protein levels (Fig. 7B). To explore whether OSBP and VAP-A play a role in the antiviral activity exerted by 25HC or 27HC, we performed target identification by siRNA sensitization (TISS) assay. This assay allows to evaluate whether knockdown of OSBP or VAP-A results in enhanced sensitivity to suboptimal concentrations of 25HC or 27HC.

Silencing of the expression of both proteins by specific siRNA improved the antiviral efficacy of both 25HC and 27HC (Fig. 8A-B-D-E). By contrast, no effect was observed when the cells were transfected with a non-targeting siRNA. A slight but significant ($p_{ANOVA} < 0.01$) block of HRV infectivity was measurable in the OSBP- and VAP-A-silenced untreated cells (Fig. 8C-F). Taken together, these results prove that OSBP and VAP-A are cellular determinants of the anti-HRV activity elicited by 25HC and 27HC.

25HC and 27HC induce cholesterol accumulation in LEs

We next investigated by confocal immunomicroscopy whether treatment of MA104 cells with 25HC or 27HC induces cholesterol accumulation in LEs. As a positive control, cells were treated with U18666A, an amphipathic steroid 3-β-[2-(diethylamine)ethoxy] androst-5-en-17-one that blocks the exit of free cholesterol from the LE compartment. Cholesterol accumulation was visualized by filipin, a fluorescent polyene antibiotic that binds to cholesterol but not to esterified sterols. As compared to the untreated cells, cholesterol accumulation was observed in the LEs of the cells treated with the oxysterols or U18666A, along with enlargement of the LE compartment (Fig. 9). Like 25HC and 27HC, U18666A was found to be endowed with anti-

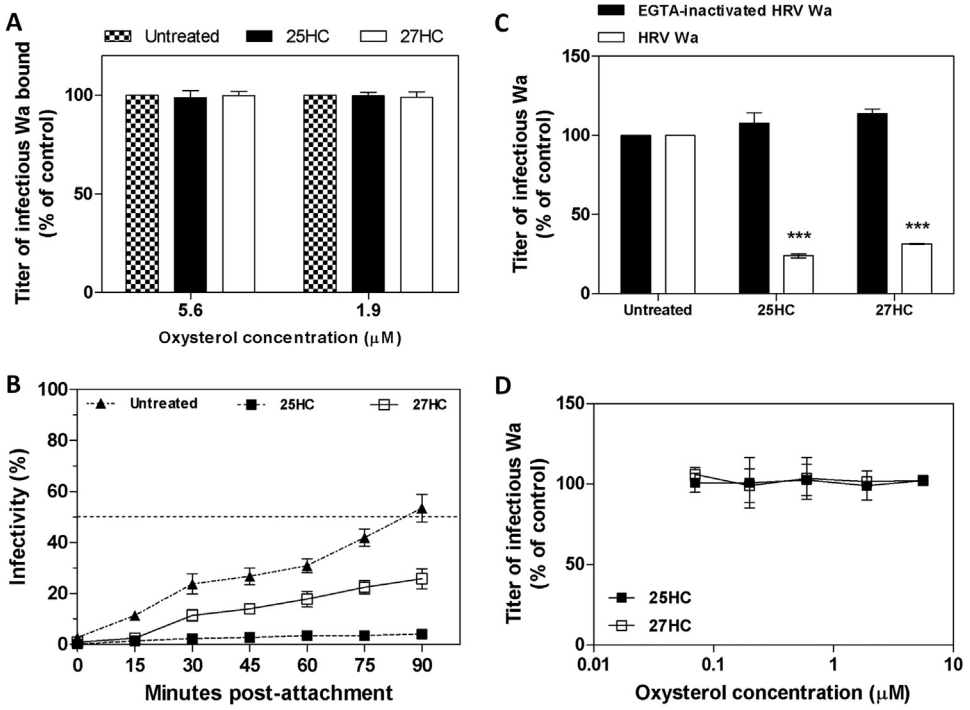

Fig. 5. Evaluation of the step of HRV inhibited by 25HC and 27HC. Panel A shows the effect of oxysterols on binding to the MA104 cell surface. On the *y* axis, the infectious titer of Wa bound to cells is expressed as a % of the titer bound to control untreated MA104 cells. Error bars represent the SEM of 3 independent experiments. Panel B: HRV Wa entry kinetics on treated or untreated MA104 cell monolayers. Virus was inoculated at 4 °C for 1 h, then temperature was shifted to 37 °C. HRV-cell penetration was stopped with EGTA in PBS at fixed time points. On the y axis, the number of infected cells in the treated or untreated samples is expressed as a percentage of infected cells when no EGTA wash was performed, which was taken as 100% entry. Each point represents mean and SEM for triplicates. Panel C: Effect of oxysterols on the infectivity of EGTA-inactivated HRV Wa transfected with lipofectamine (black bars) or trypsin-activated HRV Wa (white bars). MA104 cells were treated 20 h before inoculums. Panel D: Effect of oxysterols when added after HRV escape from LEs. Cells were infected for 45 min, treated with 25 mM of NH_4Cl for 15 min, then oxysterols were added. In panels C-D, the percentage infection was calculated by comparing treated and untreated wells. The results are means and SEM for triplicates. ***$p_{ANOVA} < 0.001$.

HRV activity (Table 3; Fig. 10A, B, C, D, E), even when the cells were infected with high MOIs (Fig. 10F), it was not endowed with antiviral activity when added after HRV escape from LEs (Fig. 10G), when cells were infected with an HRV suspension that skipped the endocytosis steps (Fig. 10H), and it blocked the viruses penetrating inside the LEs (Fig. 10I).

Discussion

Here we show that 25HC and 27HC sequester HRV Wa inside LEs and that both are endowed with antiviral activity against the LEs-dependent strains Wa, WI61, and DS-1, as well as against strains HRV248 and HRV408. Physiologic concentrations of 25HC and 27HC range from

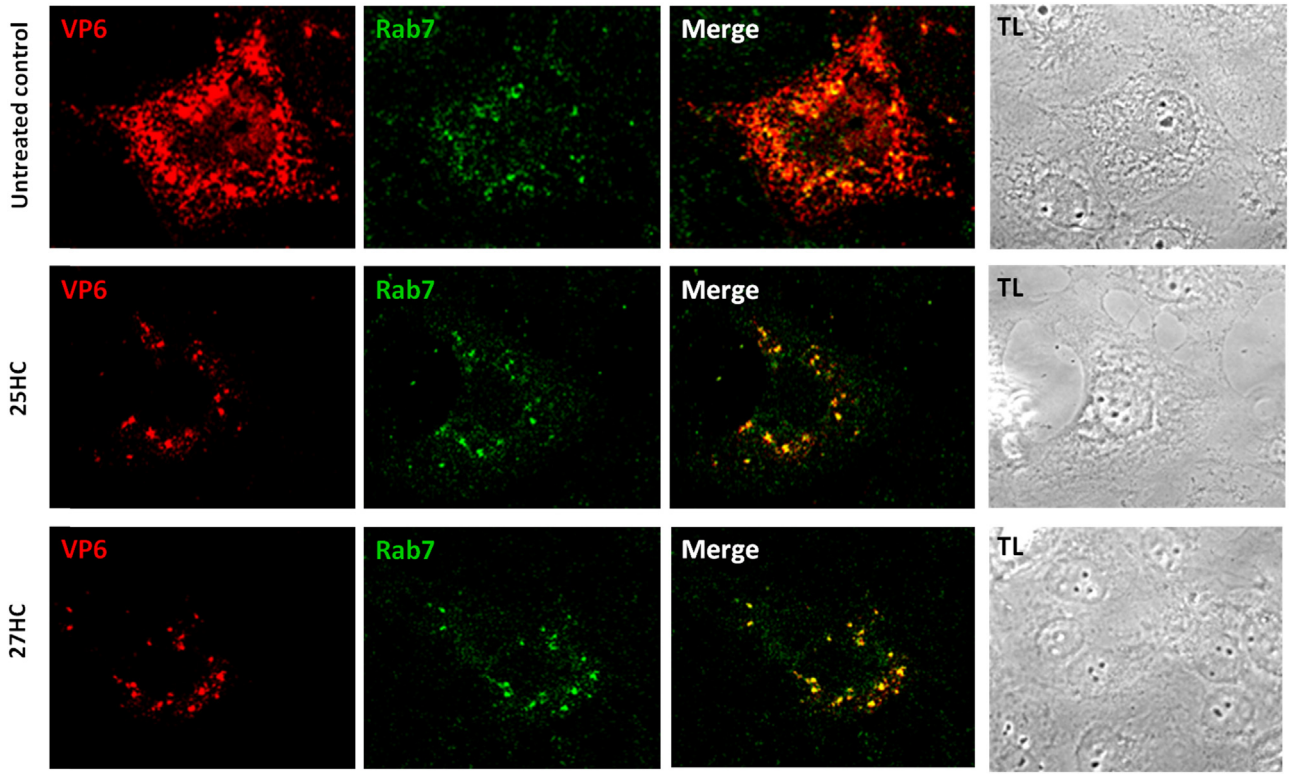

Fig. 6. Intracellular localization of HRV VP6 antigen as assessed by immunofluorescence experiments. Infected MA104 were fixed at 8 h post-infection and stained with anti-VP6 antibody (red signal) and anti-Rab7 antibody (green signal). The inserts in the right panels show the merged signals.

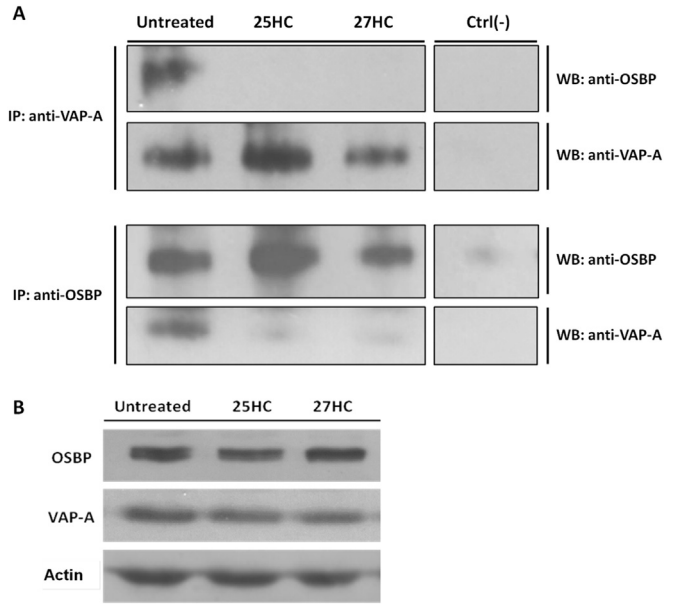

Fig. 7. Panel A: effect of 25HC or 27HC treatment on the interaction of OSBP and VAP-A, as assessed by coimmune precipitation experiments. A total amount of 500 μg of proteins extracted from treated or untreated cells was pulled-down with anti-VAP-A antibody (upper insert) or anti-OSBP antibody (lower insert) overnight at 4 °C. A control (Ctrl(-)) pull-down was performed with or anti-VP6 antibody. The precipitated proteins were analyzed by immunoblotting. IP: immune precipitation; WB: Western blot. Panel B: effect of 25HC or 27HC treatment on the expression of OSBP and VAP-A. Actin blotting was used as normalization.

1 to 25 μg/L for 25HC and from 25 to 250 μg/L for 27HC. The average EC_{50}s of 25HC against HRV strains are 0.15 μM as assessed on MA104 cells (corresponding to 60 μg/L), and 0.30 μM on Caco2 (corresponding to 121 μg/L), being at supraphysiologic levels. Notably, average EC_{50}s of 27HC are 0.36 μM on MA104 cells (corresponding to 145 μg/L), and 0.49 μM on Caco2 (corresponding to 197 μg/L), being both in the physiologic range of concentrations of this oxysterol. The intracellular localization of HRV particles was assessed in immunofluorescence experiments using a specific antibody directed to the intermediate capsid protein VP6: since this antibody does not recognize the whole TLP particle (VP6 is hidden beneath the external capsid), we can assume that the HRV particles sequestered in the LEs of the oxysterol-treated cells are DLPs. This suggests that oxysterols do not inhibit the disassembly of the HRV external capsid (which would lead to permeabilization of the LEs membrane), but rather they somehow modify the LE milieu that halts the release of DLPs from LEs. Accumulation of cholesterol within LE compartments has been shown to alter their function, significantly impairing the infection of certain enveloped viruses that enter the cell through endocytosis, such as Influenza A virus (IAV), vescicular stomatitis virus (VSV), and dengue virus [38, 40, 41].

Oxysterols are implicated in endosomal cholesterol homeostasis through their interaction with OSBP. Mammalian OSBP and OSBP-related proteins (ORPs) constitute a large eukaryotic gene family characterized by a conserved C-terminal sterol-binding domain [42]. Their primary function is to transfer cholesterol, ergosterol or oxysterols between target membranes and/or to transduce sterol-dependent signals at these points of contact [43,44]. The OSBP possess N-terminal pleckstrin homology (PH) domains that interact with phosphatidylinositol (PI) phosphates [45,46] and two phenylalanines (FF) in an acidic tract (FFAT) motif that bind the vesicle-associated membrane protein–associated protein A (VAP-A) on the cytoplasmic surface of the endoplasmic reticulum (ER; 47, 48). The complex VAP-A-OSBP mediates the transport of de novo synthesized cholesterol from the ER to other intracellular organelles.

A recent study by Amini-Bavil-Olyaee and colleagues investigating OSBP/VAP-A-mediated cholesterol shuttling as a cellular restriction mechanism of innate immunity against enveloped viruses showed that interferon-inducible transmembrane protein 3 (IFITM3) expression induces substantial accumulation of cholesterol within LE compartments in a VAP-A binding dependent manner [38]. IFITM3 was found to interact with VAP-A and prevent its association with OSBP, so inducing a marked accumulation of cholesterol in multivesicular bodies and LEs; the latter event inhibited the fusion of intraluminal virion-containing vesicles with endosomal membranes, thereby blocking virus release into the cytosol of IAV and VSV.

To this end, Tanner and Lee commented on a novel and intriguing antiviral mechanism they called “the greasy response” to viral infections: IFITM3 expressed at LE compartments interacts with VAP-A and disrupts the ER resident complex between OSBP and VAP-A, leading to cholesterol accumulation in LE, thus blocking virus entry [39]. An eventual involvement of oxysterol (the highest affinity ligands of OSBP) was never demonstrated.

In the present study, we demonstrate for the first time that oxysterols can trigger this antiviral mechanism, and that this restriction strategy can block the infectivity of a non-enveloped virus. Consistent with previous data showing 25HC-induced translocation of OSBP from the ER (where VAP-A is localized) to the Golgi [49], we show that treatment with 25HC prevents the association of OSBP to VAP-A. More interestingly, we report that even 27HC can abolish OSBP-VAP-A interaction. Accordingly, both 25HC and 27HC appeared to induce a substantial accumulation of cholesterol in the LE compartment.

In agreement with our initial hypothesis, the antiviral effect of oxysterols was potentiated in the cells in which the expression of either OSBP or VAP-A was silenced. The silencing of these proteins in the untreated cells exerted a partial block of HRV infectivity, thus stressing the involvement of these two proteins in HRV replication.

The present report also provides proof of concept that accumulation of cholesterol within LEs is an effective anti-HRV mechanism. While many studies have demonstrated the wide spectrum of antiviral activity of U18666A against enveloped viruses [50–52], we provide the first evidence of its antiviral potential against a non-enveloped virus. This cationic amphiphile causes a significant block of HRV infectivity even at high MOIs by inducing cholesterol accumulation on LEs and sequestering HRV inside them. This finding opens the way to the search for small anti-HRV molecules endowed with this molecular mechanism.

Cholesterol accumulation on the membrane of LEs leads to several dramatic modifications of this intracellular compartment. Our results show that cholesterol accumulation in the larger cholesterol-enriched LEs in the 25HC-, 27HC-, and U18666A-treated cells leads to enlargement of LEs. Moreover, Sobo and colleagues showed that cholesterol accumulation dramatically perturbs the back fusion of intraluminal vesicles with the limiting membrane and intra-organellar trafficking [53]. Inhibition of back fusion events is expected to severely interfere with the sorting and trafficking of the proteins that cycle between intraluminal and limiting membranes, as was shown for the cation-dependent mannose-6-phosphate receptor (CD-M6PR; 53). LE-dependent HRVs are strictly dependent on the presence of the CD-M6PR on such vesicles to become uncoated and exit the endosomal system [37]. These cholesterol-induced perturbations of the LE compartment provide a reasonable explanation for why cholesterol accumulation blocks HRV particles inside these organelles.

In conclusion, both 25HC and 27HC appear to exert a remarkable anti-HRV effect, based at least on the impairment of the OSBP/VAP-A interplay and on abnormal cholesterol accumulation within LEs, the last gate for the virus to enter the cytosol. Indeed, since these side chain oxysterols have been shown to drive a number of biochemical reactions within the cells [14], their direct action on LE structure and function cannot be excluded.

This study discloses a totally novel mechanism of two oxysterols of enzymatic origin suggesting that, besides 25HC, other members of this

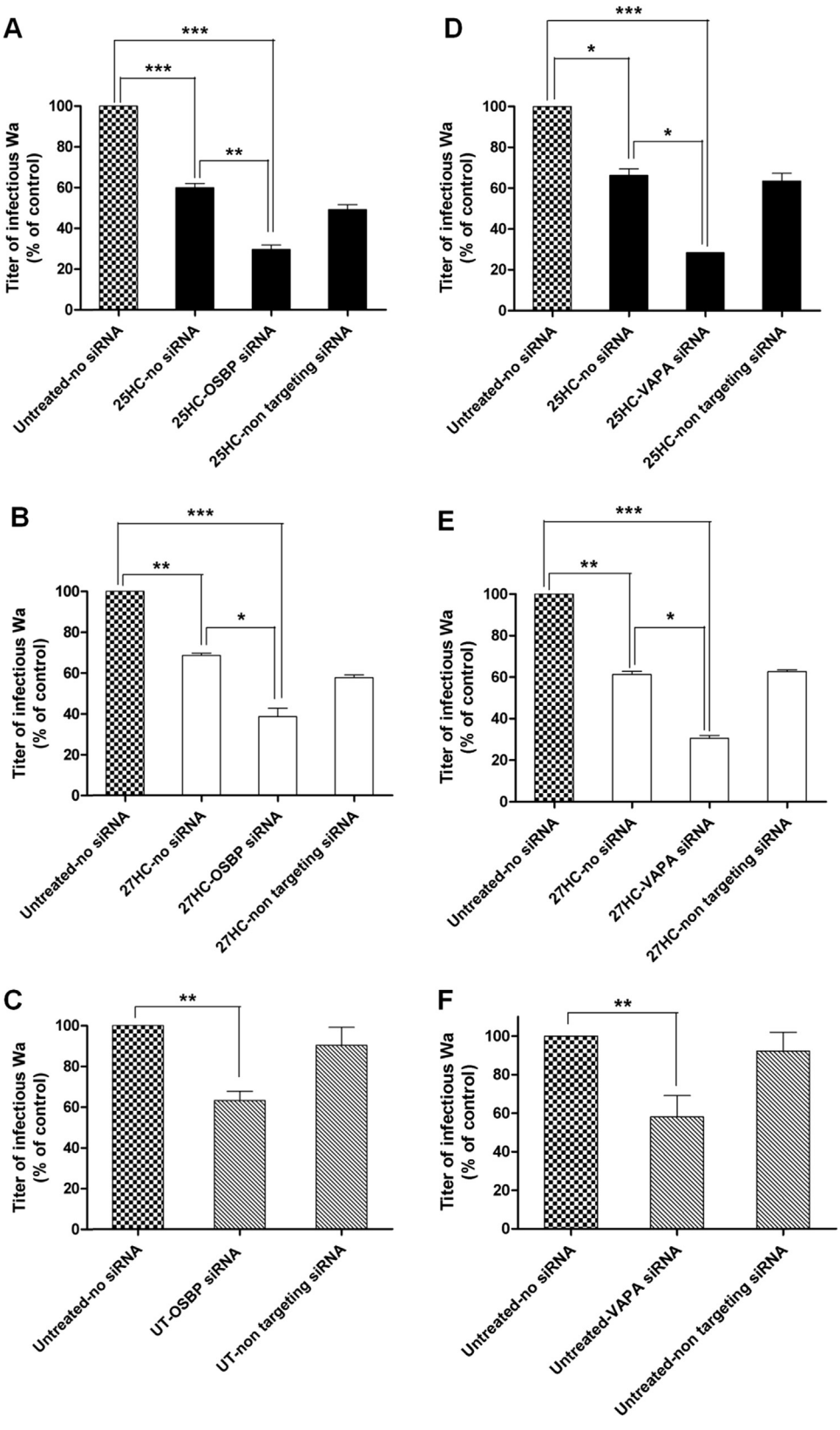

Fig. 8. Effect of OSBP silencing (panels A, B, and C) or VAP-A silencing (panels D, E, and F) by short interfering RNA (siRNA) transfection on the antiviral activity of 25HC or 27HC. Cells were transfected for 72 h with 20 nM of anti-OSBP siRNA, anti-VAP-A siRNA or control non-interfering siRNA. Cells were then treated for 20 h with oxysterols at sub-optimal concentrations and finally infected with HRV Wa. Viral infections were detected as described in the Material and Methods section. The infectivity titers of virus in the treated samples are expressed as a percentage of the titer obtained in the absence of treatment. Error bars represent the standard error of the mean (SEM) of 3 independent experiments.*$p_{ANOVA} < 0.05$; **$p_{ANOVA} < 0.01$; ***$p_{ANOVA} < 0.001$.

family could be actively involved in the innate immunity response against viruses. To these end, our results demonstrate that lipid involvement as host restriction strategy is an area of focus which, with the recent advances in technology, holds great promise to discover novel mechanisms and redox active lipid factors to develop innovative approaches for antiviral therapy.

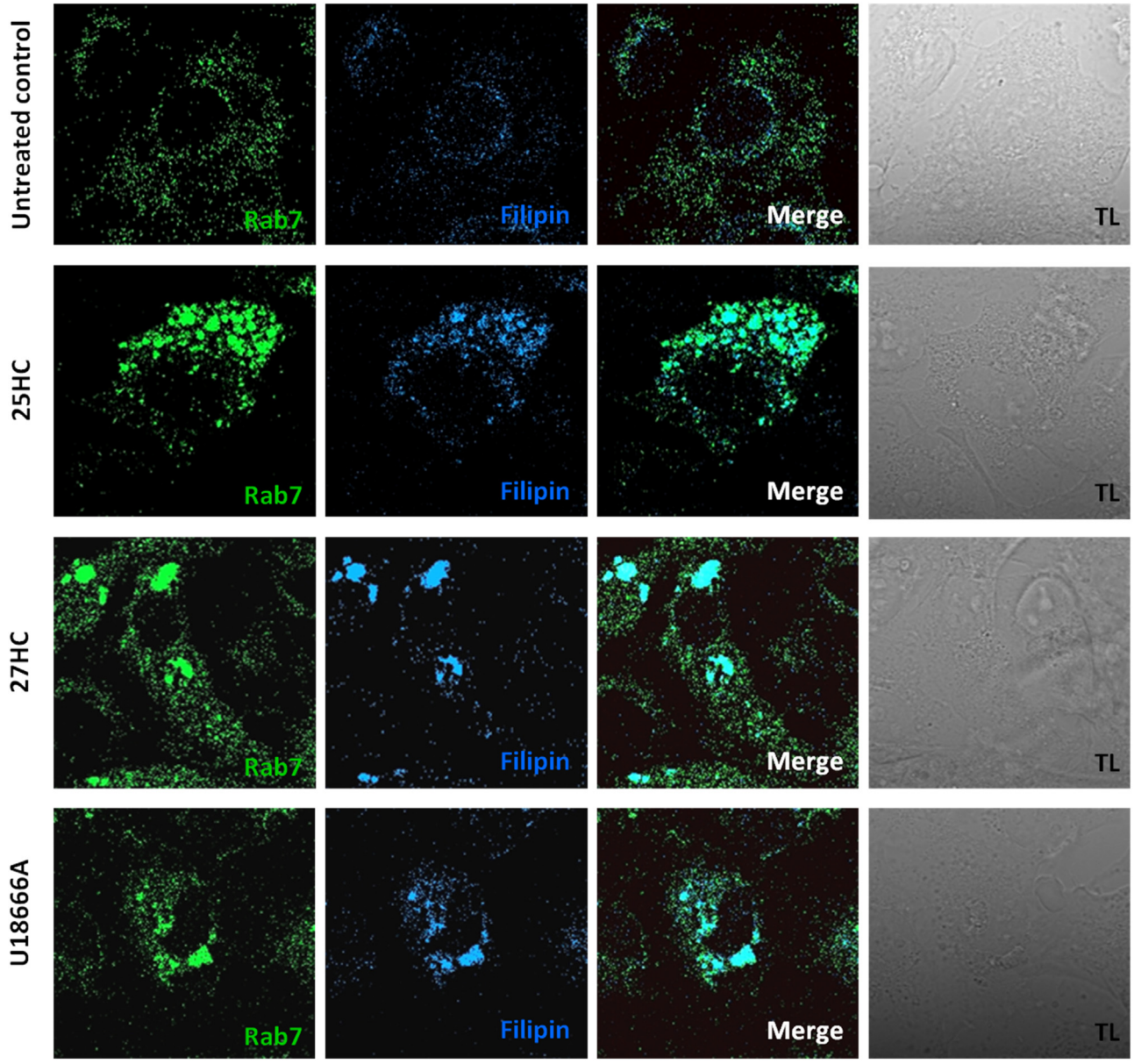

Fig. 9. Effect of 25HC or 27HC on intracellular localization of cholesterol. Positive control experiments were performed by treating cells with U18666A. Treated or untreated MA104 were fixed at 20 h post-treatment and intracellular cholesterol was stained with filipin (blue signal)and late endosomes with anti-Rab7 antibody (green signal). The inserts in the right panels show the merged signals.

Table 3
Antirotavirus activity of U18666A (MA104 cells).

Treatment	HRV strain	EC_{50}[a] (μM) – 95% CI[b]	EC_{90}[c] (μM) – 95% CI	CC_{50}[d] (μM) –95% CI	SI[e]
U18666A	Wa	1.44 (1.17–1.78)	11.66 (7.63–17.83)	219.3 (180.6–266.4)	152.29
	WI61	7.84 (7.08–8.68)	20.89 (16.72–26.09)	219.3 (180.6–266.4)	27.97
	HRV408	2.14 (1.55–2.95)	12.04 (5.94–24.42)	219.3 (180.6–266.4)	102.47
	HRV248	2.63 (1.74–3.80)	17.60 (7.05–43.94)	219.3 (180.6–266.4)	83.38
	DS-1	5.84(4.76–7.16)	19.87 (12.43–31.74)	219.3 (180.6–266.4)	37.56

n.a. not assessable.
[a] EC_{50} half-maximal effective concentration.
[b] CI confidence interval.
[c] EC_{90}90% effective concentration.
[d] CC_{50} half maximal cytotoxic concentration.
[e] SI selectivity index.

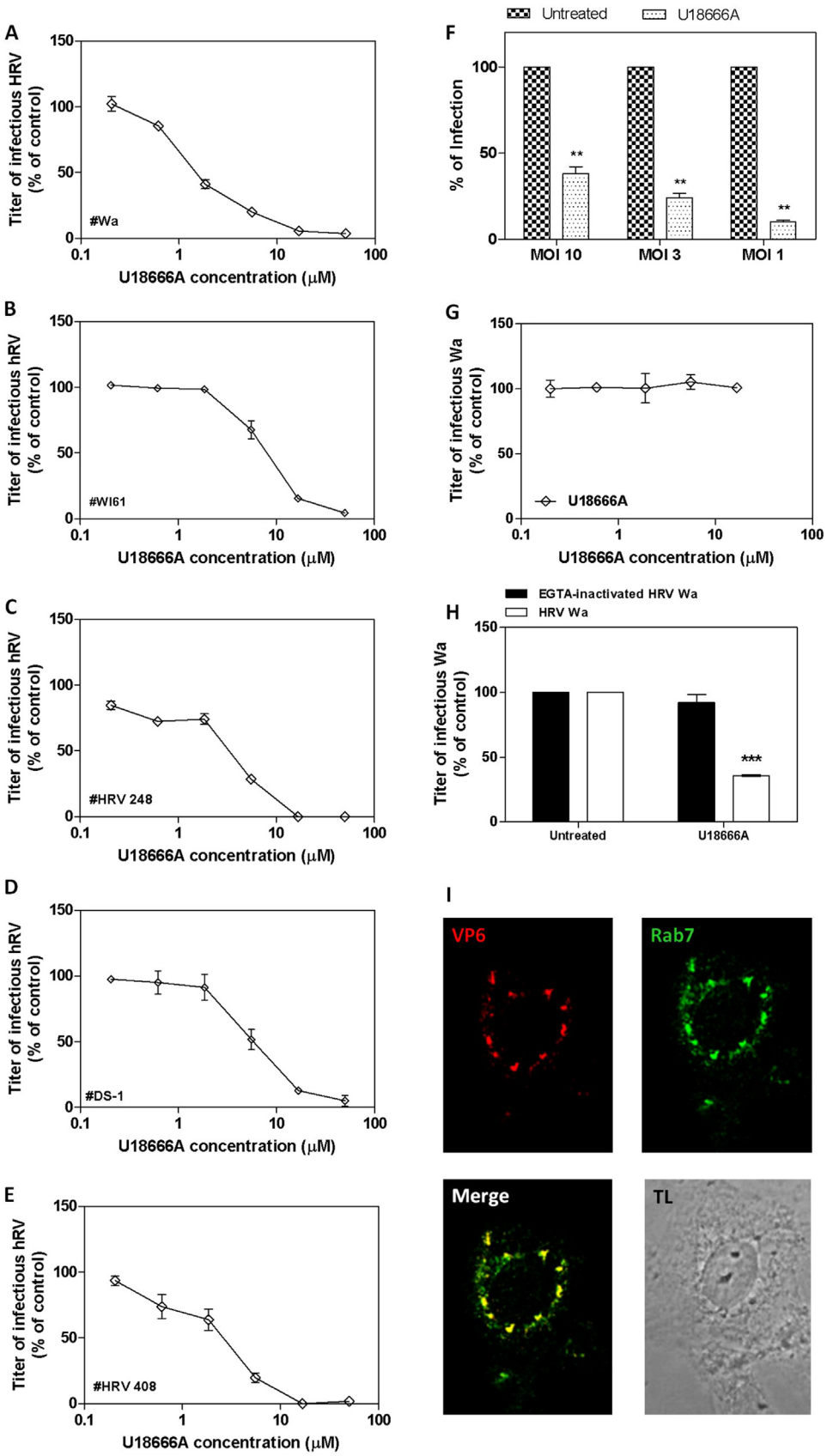

Fig. 10. Assessment of the antiviral activity of U18666A against HRV strains and assessment of its mechanism of action. Cells were treated for 20 h with increasing concentrations of U18666A and then infected with HRV Wa (A), WI61 (B), HRV 248 (C), DS-1 (D), and HRV 408 (E). Viral infections were detected as described in the Material and Methods section. The percentage infection was calculated by comparing treated and untreated wells. The results are means and SEM for triplicates.***$p_{ANOVA} < 0.001$. Panel F: cells were treated with 1.9 μM of U18666A for 20 h, then infected with high multiplicities of infection (MOIs) of HRV Wa. The percentage infection was calculated by comparing treated and untreated wells. The results are means and SEM for triplicates.**$p_{ANOVA} < 0.01$. Panel G: effect of oxysterols when added after HRV escape from LEs. Cells were infected for 45 min, treated with 25 mM of NH_4Cl for 15 min, then oxysterols were added. Panel H: effect of oxysterols on the infectivity of EGTA-inactivated HRV Wa transfected with lipofectamine (black bars) or trypsin-activated HRV Wa (white bars). MA104 cells were treated 20 h before inoculums. * **$p_{ANOVA} < 0.001$ Panel I: intracellular localization of HRV VP6 antigen as assessed by immunofluorescence experiments. Infected MA104 were fixed at 8 h post-infection and stained with anti-VP6 antibody (red signal) and anti-Rab7 antibody (green signal). The inserts in the right panels show the merged signals.

Materials and methods

Cell line and viruses

African green monkey kidney epithelial cells (MA104) and human epithelial colorectal adenocarcinoma cells (Caco-2) were propagated in Dulbecco's Modified Eagle Medium (DMEM; Sigma, St. Louis, MO, USA) supplemented with 1% (v/v) Zell Shield (Minerva Biolabs, Berlin, Germany) and heat inactivated, 10% (v/v) fetal bovine serum (Sigma). Human rotavirus (HRV) strains Wa (ATCC® VR-2018), WI61 (ATCC® VR-2551), HRV 408 (ATCC® VR-2273), HRV 248 (ATCC® VR-2274), DS-1 (ATCC® VR-2550) were purchased from ATCC (American Type Culture Collection, Rockville, MD, USA); virus was activated with 5 μg/ml of porcine pancreatic trypsin type IX (Sigma) for 30 min at 37 °C and propagated in MA104 cells using DMEM containing 0.5 μg of trypsin per ml as described previously [54]. Viral titers are expressed as focus-forming unit (FFU) per ml.

Antibodies and reagents

25HC and 27HC (Sigma) were dissolved in sterile ethanol at concentrations ranging from 2.75 mM to 3 mM. U18666A was purchased from Millipore (Darmstadt, Germany) and dissolved in sterile dimethyl sulfoxide (DMSO) to a concentration of 5 mM. Mouse monoclonal antibody (MAb) directed to human rotavirus VP6 (2B4) was purchased from Covalab (Villeurbanne, France). The rabbit polyclonal antibodies directed to VAP-A (H-40: sc-98890) and Rab 7 (H-50: sc-10767) were purchased from Santa Cruz Biotechnology, Inc. (Dallas, TX, USA). The rabbit polyclonal antibody directed to OSBP (C2C3) was purchased from GeneTex (Irvine, CA, USA). The rabbit polyclonal antibody to OSBP-N-terminal (ab192990) was purchased from Abcam (Cambridge, UK). The mouse monoclonal antibody directed to actin (MAB1501R) was purchased from Millipore. The secondary antibody peroxidase-conjugated AffiniPure F(ab')2 Fragment Goat Anti-Mouse IgG (H + L) was purchased from Jackson ImmunoResearch Laboratories Inc. (West Grove, PA, USA). The secondary antibodies anti-mouse IgG horseradish (HRP)-linked (NA931V) and anti-rabbit IgG HRP-linked (NA934V) were purchased from GE Healthcare UK (Chalfont St Giles, UK). The secondary antibodies goat anti-rabbit IgG-FITC (sc-2012) and goat anti-mouse IgG-R (sc-2092) were purchased from Santa Cruz Biotechnology, Inc.

Antiviral assays

The antiviral efficacy of the oxysterols was determined by focus reduction assay on confluent MA104 or Caco2 cell monolayers plated in 96-well trays, as described elsewhere [21]. Cells were treated for 20 h at 37 °C with 25HC, 27HC or U18666A at concentrations ranging from 0.07 to 16.7 μM (corresponding to 28.2 and 6724 μg/L for both oxysterols, and 29.7 and 7082 μg/L for U18666A). Control samples (100% of infectivity) were prepared by treating cells with culture medium supplemented with equal volumes of ethanol or DMSO, corresponding to 0.6% (v/v) to 0.0014% (v/v) in cell media. Cells were then washed with medium and infected with HRV at a multiplicity of infection (MOI) of 0.02 FFU/cell for 1 h, unless otherwise stated. Alternatively, MA104 cells were treated for 20 h with 25HC, 27HC, or U18666A at respective EC90 concentrations and then infected for 1 h with HRV Wa at MOIs 10, 3, and 1. Experiments with EGTA-inactivated HRV were performed by treating trypsin activated HRV Wa for 15 min with 1.5 mM EGTA at room temperature. Infection was then performed for 1 h at 37 °C in presence of Lipofectamine (Invitrogen Carlsbad, CA). This technique represents a useful strategy to skip viral penetration through endocytosis while delivering in cytoplasm HRV DLPs ready to start viral RNA transcription [55]. After infection, cells were washed with medium and incubated at 37 °C in a humidified incubator in 5% (vol/vol) CO_2–95% (vol/vol) air until fixed. For time-of-addition assays, serial dilutions of oxysterols were added on cells alternatively 20 h or 4 h before infection or during infection or post-infection. Alternatively, cells were infected with trypsin-activated HRV Wa for 45 min at 37 °C, then medium supplemented with 25 mM NH_4Cl was added. This technique inhibits endosome acidification thereby sequestering HRV particles that are still inside the endosomes, while permitting the replication of those that already escaped from LEs [56]. After 15 min of incubation at 37 °C, oxysterols in presence of 25 mM NH_4Cl were added. After each one of these treatment/infection protocols, cells were incubated for 16 h, then fixed with cold acetone-methanol (50:50), and viral titers were determined by indirect immunostaining. Blockade of viral infectivity is expressed as mean % ± standard error of the mean (SEM).

Cell viability assay

Cells were seeded at a density of 5×10^3/well in 96-well plates and treated the next day with oxysterols 25HC, 27HC, or U18666A at concentrations ranging from 0.07 to 150 μM (corresponding to 28.2 and 60400 μg/L for both oxysterols, and 29.7 and 63609 μg/L for U18666A) to generate dose-response curves. Control samples (100% of viability) were prepared by treating cells with culture medium supplemented with equal volumes of ethanol, corresponding to 0.6% (v/v) to 0.0025% (v/v) in cell media. After 24 h of incubation, cell viability was determined using a CellTiter 96 Proliferation Assay Kit (Promega, Madison, WI, USA) and following the manufacturer's instructions. Absorbances were measured using a Microplate Reader (Model 680, Bio-Rad Laboratories, Hercules, CA, USA) at 490 nm. Viability of oxysterol-treated cells is expressed as a percentage relative to cells incubated with culture medium supplemented with equal volumes of ethanol.

Rotavirus-cell binding assay

Rotavirus-cell binding assays were performed as described previously [54]. Confluent MA104 cell monolayers in 24-well trays were treated with 25HC or 27HC at 1.8 μM or 5.6 μM. After 20 h, cells were washed with fresh medium and cooled on ice. Trypsin-activated virus, which had been cooled to 4 °C, was allowed to attach to cells for 1 h (MOI = 3 FFU/cell) at 4 °C. After a washing with cold DMEM, the cells were subjected to two rounds of freeze-thawing and then incubated at 37 °C for 30 min with 10 μg/ml porcine trypsin to release bound virus. The lysates were clarified by low speed centrifugation for 10 min. Cell-bound virus titers were determined by indirect immunostaining as above.

Rotavirus-cell entry assay

Confluent MA104 cell monolayers in 96-well plates were treated with 25HC or 27HC at concentrations ranging from 0.07 to 16.7 μM. After 20 h, cells were washed twice with DMEM and cooled on ice for 20 min. Trypsin-activated virus, which had been cooled to 4 °C, was adsorbed to cells on ice for 1 h at 4 °C (MOI = 0.2 FFU/cell) to ensure virus attachment but not entry. Unbound viruses were then washed, warmed medium was added, and the plates were incubated at 37 °C in humidified atmosphere to allow entry. At fixed timepoints (0, 15, 30, 45, 60, 75, 90 min after virus-cell attachment), the medium in the wells was aspirated, and viral particles still present on the cell surface were detached by two quick washes with 3 mM EGTA in PBS, followed by incubation in warm medium. After reaching the last timepoint (90 min), the plates were placed into a CO2 incubator, and the infection was left to proceed for an additional 16 h. The cells were then fixed and stained by indirect immunostaining as described above. The amount of virus that entered at each time point was compared to the amount of virus that entered when no EGTA wash was performed, which was taken as 100% entry.

Immunoblotting

Cells were lysed in denaturating conditions, unless otherwise stated. Extracted proteins were denatured by boiling for 5 min, then separated by sodium dodecyl sulfate–12% polyacrylamide gel electrophoresis (SDS-12% PAGE) and transferred to a polyvinylidene difluoride (PVDF) membrane. Membranes were blocked overnight at 4 °C with PBS, 0.1% Tween 20, and milk powder 10%. Membranes were then incubated with primary antibodies for 1 h at 37 °C, washed 4 times with PBS, 0.1% Tween 20, and 15% milk powder, then incubated for 1 h at 37 °C with secondary antibodies coupled with HRP and washed extensively prior to developing by the enhanced chemiluminescence method. The band density was compared using ImageJ software, and the intensity of the actin bands was used to normalize values. Where possible, the results are expressed as a percentage, by comparing treated cells with cells incubated with culture medium alone.

Immunofluorescence experiments

Subconfluent MA104 cell monolayers plated on coverslips in 24-well plates were treated with 25HC, 27HC or U18666A at 1.8 μM. After 20 h, cells were infected with trypsin-activated rotavirus Wa (MOI = 10 FFU/cell) for 8 h at 37 °C. Cells were washed twice with PBS and then fixed in cold acetone-methanol (50:50). Cells were blocked with 1% BSA for 30 min and then incubated with primary antibodies diluted in blocking buffer for 1 h followed by three washes in PBS with 0.05% Tween 20 and incubation with secondary antibodies diluted in blocking buffer for 1 h. After washing three times with PBS, coverslips were mounted and analyzed on a confocal fluorescence microscope (LSM510, Carl Zeiss, Jena, Germany).

Co-immunoprecipitation experiments

MA104 cells were treated with 5.6 μM of 25HC or 27HC for 2 h at 37 °C and then lysed in non-denaturating conditions (Tris HCl pH8 20 mM, NaCl 137 mM, NP40 1%, EDTA 2 mM, and 1X protease inhibitor mixture). The extracted proteins (500 μg) were incubated with 0.5 μg of VAP-A antibody, rabbit polyclonal to OSBP-N-terminal or anti-VP6 antibody overnight at 4 °C. Protein A-Sepharose (15 μl in PBS with 0.1% Triton X-100) was added for 1 h at 4 °C. Sepharose beads were collected by centrifugation and washed four times with 1 ml of PBS containing 1% NP40. The samples were heated to 97 °C in SDS sample buffer, separated by SDS-PAGE, and analyzed by immunoblotting.

siRNA transfection experiments

Caco2 cells (2×10^4) were transfected with 20 nM of siRNA against OSBP, VAP-A or with control non-interfering siRNAs. Each sample of transfected or untransfected cells was seeded in different wells in a 24-well tray and cultured for 72 h at 37 °C (5% CO_2). Cells were treated with suboptimal concentrations (EC_{50}) of 25HC or 27HC for 20 h, and then infected with HRV Wa (MOI 0.02 FFU/cell) as previously described. After 16 h, cells were fixed and subjected to indirect immunostaining to assess blockade of virus infectivity.

Quantitative real-time reverse transcription (RT)-PCR

The levels of siRNA-mediated silencing of OSBP or VAP-A expression were assessed by quantitative real-time reverse transcription (RT)-PCR. Briefly, extraction of total RNA from transfected or untransfected Caco2 cells was performed 72 h after transfection using TRIzol Reagent (Applied Biosystems, Monza, Italy). Concentration and purity of the extracted RNA were assessed by spectrophotometry (A260/A280). Later, 2 μg of RNA were reverse transcribed by using a High-Capacity cDNA Reverse Transcription Kit (Applied Biosystems). Quantitative RT-PCR was performed with 30 ng of cDNA using TaqMan Gene Expression Assay kits for OSBP and β-actin, TaqMan Fast Universal PCR Master Mix, and 7500 Fast Real-Time PCR System (Applied Biosystems). For each gene, threshold cycles (Ct) were determined and results were normalized using β-actin. Relative quantification was performed using a previously published mathematical method [57].

Statistical analysis

Where possible, half-maximal antiviral effective concentration (EC_{50}) values were calculated by regression analysis using the dose-response curves generated from the experimental data using GraphPad PRISM 7 (GraphPad Software, San Diego, CA, USA). The 50% cytotoxic concentration (CC_{50}) was determined using logarithmic viability curves. Where possible, a selectivity index (SI) was calculated by dividing the CC_{50} by the EC_{50} value. EC_{50} values were compared using the sum-of-squares F test. One-way ANOVA, followed by Bonferroni test, was used to assess the statistical significance of the differences between treated and untreated samples, where appropriate. Significance was set at the 95% level.

Acknowledgements

The authors' work was supported by a grant from Ricerca Locale Finanziata dall'Università degli Studi di Torino, Grant number: RILO2015 and by Fondazione CRT, Grant number: 2015.2662.

References

[1] M. Blanc, W.Y. Hsieh, K.A. Robertson, K.A. Kropp, T. Forster, G. Shui, P. Lacaze, S. Watterson, S.J. Griffiths, N.J. Spann, A. Meljon, S. Talbot, K. Krishnan, D.F. Covey, M.R. Wenk, M. Craigon, Z. Ruzsics, J. Haas, A. Angulo, W.J. Griffiths, C.K. Glass, Y. Wang, P. Ghazal, The transcription factor STAT-1 couples macrophage synthesis of 25-hydroxycholesterol to the interferon antiviral response, Immunity 38 (2013) 106–118.
[2] S.Y. Liu, R. Aliyari, K. Chikere, G. Li, M.D. Marsden, J.K. Smith, O. Pernet, H. Guo, R. Nusbaum, J.A. Zack, A.N. Freiberg, L. Su, B. Lee, G. Cheng, Interferon-inducible cholesterol-25-hydroxylase broadly inhibits viral entry by production of 25-hydroxycholesterol, Immunity 38 (2013) 92–105.
[3] S.Y. Bah, P. Dickinson, T. Forster, B. Kampmann, P. Ghazal, Immune oxysterols: role in mycobacterial infection and inflammation, J. Steroid Biochem. Mol. Biol. 169 (2017) 152–163.
[4] G. Leonarduzzi, B. Sottero, G. Poli, Oxidized products of cholesterol: dietary and metabolic origin, and proatherosclerotic effects, J. Nutr. Biochem. 13 (2002) 700–710.
[5] G. Leonarduzzi, P. Gamba, B. Sottero, A. Kadl, F. Robbesyn, R.A. Calogero, F. Biasi, E. Chiarpotto, N. Leitinger, A. Sevanian, G. Poli, Oxysterol-induced up-regulation of MCP-1 expression and synthesis in macrophage cells, Free Radic. Biol. Med. 39 (2005) 1152–1161.
[6] V. Mutemberezi, O. Guillemot-Legris, G.G. Muccioli, Oxysterols: from cholesterol metabolites to key mediators, Prog. Lipid Res. 64 (2016) 152–169.
[7] V. Luu-The, Assessment of steroidogenesis and steroidogenic enzyme functions, J. Steroid Biochem. Mol. Biol. 137 (2013) 176–182.
[8] T. Jakobsson, E. Treuter, J.A. Gustafsson, K.R. Steffensen, Liver X receptor biology and pharmacology: new pathways, challenges and opportunities, Trends Pharmacol. Sci. 33 (2012) 394–404.
[9] R. Lappano, A.G. Recchia, E.M. De Francesco, T. Angelone, M.C. Cerra, D. Picard, M. Maggiolini, The cholesterol metabolite 25-hydroxycholesterol activates estrogen receptor alpha-mediated signaling in cancer cells and in cardiomyocytes, PLoS One 6 (2011) e16631.
[10] L. Raccosta, R. Fontana, D. Maggioni, C. Lanterna, E.J. Villablanca, A. Paniccia, A. Musumeci, E. Chiricozzi, M.L. Trincavelli, S. Daniele, C. Martini, J.A. Gustafsson, C. Doglioni, S.G. Feo, A. Leiva, M.G. Ciampa, L. Mauri, C. Sensi, A. Prinetti, I. Eberini, J.R. Mora, C. Bordignon, K.R. Steffensen, S. Sonnino, S. Sozzani, C. Traversari, V. Russo, The oxysterol-CXCR2 axis plays a key role in the recruitment of tumor-promoting neutrophils, J. Exp. Med. 210 (2013) 1711–1728.
[11] A. Radhakrishnan, Y. Ikeda, H.J. Kwon, M.S. Brown, J.L. Goldstein, Sterol-regulated transport of SREBPs from endoplasmic reticulum to Golgi: oxysterols block transport by binding to Insig, Proc. Natl. Acad. Sci. USA 104 (2007) 6511–6518.
[12] R.E. Infante, L. Abi-Mosleh, A. Radhakrishnan, J.D. Dale, M.S. Brown, J.L. Goldstein, Purified NPC1 protein. I. Binding of cholesterol and oxysterols to a 1278-amino acid membrane protein, J. Biol. Chem. 283 (2008) 1052–1063.
[13] V.M. Olkkonen, S. Li, Oxysterol-binding proteins: sterol and phosphoinositide sensors coordinating transport, signaling and metabolism, Prog. Lipid Res. 52 (2013) 529–538.
[14] B. Vurusaner, G. Leonarduzzi, P. Gamba, G. Poli, H. Basaga, Oxysterols and mechanisms of survival signaling, Mol. Asp. Med. 49 (2016) 8–22.
[15] C. Moog, A.M. Aubertin, A. Kirn, B. Luu, Oxysterols, but not cholesterol, inhibit

human immunodeficiency virus replication in vitro, Antivir. Chem. Chemother. 9 (1998) 491–496.
[16] E.S. Gold, A.H. Diercks, I. Podolsky, R.L. Podyminogin, P.S. Askovich, P.M. Treuting, A. Aderem, 25-Hydroxycholesterol acts as an amplifier of inflammatory signaling, Proc. Natl. Acad. Sci. USA 111 (2014) 10666–10671.
[17] A.I. Su, J.P. Pezacki, L. Wodicka, A.D. Brideau, L. Supekova, R. Thimme, S. Wieland, J. Bukh, R.H. Purcell, P.G. Schultz, F.V. Chisari, Genomic analysis of the host response to hepatitis C virus infection, Proc. Natl. Acad. Sci. USA 99 (2002) 15669–15674.
[18] M. Iwamoto, K. Watashi, S. Tsukuda, H.H. Aly, M. Fukasawa, A. Fujimoto, R. Suzuki, H. Aizaki, T. Ito, O. Koiwai, H. Kusuhara, T. Wakita, Evaluation and identification of hepatitis B virus entry inhibitors using HepG2 cells overexpressing a membrane transporter NTCP, Biochem. Biophys. Res. Commun. 443 (2014) 808–813.
[19] V. Cagno, A. Civra, D. Rossin, S. Calfapietra, C. Caccia, V. Leoni, N. Dorma, F. Biasi, G. Poli, D. Lembo, Inhibition of herpes simplex-1 virus replication by 25-hydroxycholesterol and 27-hydroxycholesterol, Redox Biol. 12 (2017) 522–527.
[20] M. Arita, H. Kojima, T. Nagano, T. Okabe, T. Wakita, H. Shimizu, Oxysterol-binding protein family I is the target of minor enviroxime-like compounds, J. Virol. 87 (2013) 4252–4260.
[21] A. Civra, V. Cagno, M. Donalisio, F. Biasi, G. Leonarduzzi, G. Poli, D. Lembo, Inhibition of pathogenic non-enveloped viruses by 25-hydroxycholesterol and 27-hydroxycholesterol, Sci. Rep. 4 (2014) 7487.
[22] P.S. Roulin, M. Lötzerich, F. Torta, L.B. Tanner, F.J. van Kuppeveld, M.R. Wenk, U.F. Greber, Rhinovirus uses a phosphatidylinositol 4-phosphate/cholesterol counter-current for the formation of replication compartments at the ER-Golgi interface, Cell Host Microbe 16 (2014) 677–690.
[23] J.G. Cyster, E.V. Dang, A. Reboldi, T. Yi, 25-Hydroxycholesterols in innate and adaptive immunity, Nat. Rev. Immunol. 14 (2014) 731–743.
[24] D. Lembo, V. Cagno, A. Civra, G. Poli, Oxysterols: an emerging class of broad spectrum antiviral effectors, Mol. Asp. Med. 49 (2016) 23–30.
[25] S.M. Sagan, Y. Rouleau, C. Leggiadro, L. Supekova, P.G. Schultz, A.I. Su, J.P. Pezacki, The influence of cholesterol and lipid metabolism on host cell structure and hepatitis C virus replication, Biochem. Cell Biol. 84 (2006) 67–79.
[26] C. Wang, M. Gale Jr., B.C. Keller, H. Huang, M.S. Brown, J.L. Goldstein, J. Ye, Identification of FBL2 as a geranylgeranylated cellular protein required for hepatitis C virus RNA replication, Mol. Cell 18 (2005) 425–434.
[27] J. Ye, C. Wang, R. Sumpter Jr., M.S. Brown, J.L. Goldstein, M. Gale Jr., Disruption of hepatitis C virus RNA replication through inhibition of host protein geranylgeranylation, Proc. Natl. Acad. Sci. USA 100 (2003) 15865–15870.
[28] J.P. Pezacki, S.M. Sagan, A.M. Tonary, Y. Rouleau, S. Bélanger, L. Supekova, A.I. Su, Transcriptional profiling of the effects of 25-hydroxycholesterol on human hepatocyte metabolism and the antiviral state it conveys against the hepatitis C virus, BMC Chem. Biol. 9 (2009) 2.
[29] K.L. Kotloff, J.P. Nataro, W.C. Blackwelder, D. Nasrin, T.H. Farag, S. Panchalingam, Y. Wu, S.O. Sow, D. Sur, R.F. Breiman, A.S. Faruque, A.K. Zaidi, D. Saha, P.L. Alonso, B. Tamboura, D. Sanogo, U. Onwuchekwa, B. Manna, T. Ramamurthy, S. Kanungo, J.B. Ochieng, R. Omore, J.O. Oundo, A. Hossain, S.K. Das, S. Ahmed, S. Qureshi, F. Quadri, R.A. Adegbola, M. Antonio, M.J. Hossain, A. Akinsola, I. Mandomando, T. Nhampossa, S. Acácio, K. Biswas, C.E. O'Reilly, E.D. Mintz, L.Y. Berkeley, K. Muhsen, H. Sommerfelt, R.M. Robins-Browne, M.M. Levine, Burden and aetiology of diarrhoeal disease in infants and young children in developing countries (the Global Enteric Multicenter Study, GEMS): a prospective, case-control study, Lancet 382 (2013) 209–222.
[30] A.L. Shaw, R. Rothnagel, C.Q. Zeng, J.A. Lawton, R.F. Ramig, M.K. Estes, B.V. Prasad, Rotavirus structure: interactions between the structural proteins, Arch. Virol. Suppl. 12 (1996) 21–27.
[31] M. Yeager, J.A. Berriman, T.S. Baker, A.R. Bellamy, Three-dimensional structure of the rotavirus haemagglutinin VP4 by cryo-electron microscopy and difference map analysis, EMBO J. 13 (1994) 1011–1018.
[32] K.L. Graham, P. Halasz, Y. Tan, M.J. Hewish, Y. Takada, E.R. Mackow, M.K. Robinson, B.S. Coulson, Integrin-using rotaviruses bind alpha2beta1 integrin alpha2 I domain via VP4 DGE sequence and recognize alphaXbeta2 and alphaVbeta3 by using VP7 during cell entry, J. Virol. 77 (2003) 9969–9978.
[33] J.E. Ludert, N. Feng, J.H. Yu, R.L. Broome, Y. Hoshino, H.B. Greenberg, Genetic mapping indicates that VP4 is the rotavirus cell attachment protein in vitro and in vivo, J. Virol. 70 (1996) 487–493.
[34] D.M. Bass, E.R. Mackow, H.B. Greenberg, Identification and partial characterization of a rhesus rotavirus binding glycoprotein on murine enterocytes, Virology 183 (1991) 602–610.
[35] C.D. Kirkwood, R.F. Bishop, B.S. Coulson, Attachment and growth of human rotaviruses RV-3 and S12/85 in Caco-2 cells depend on VP4, J. Virol. 72 (1998) 9348–9352.
[36] M.A. Díaz-Salinas, D. Silva-Ayala, S. López, C.F. Arias, Rotaviruses reach late endosomes and require the cation-dependent mannose-6-phosphate receptor and the activity of cathepsin proteases to enter the cell, J. Virol. 88 (2014) 4389–4402.
[37] E.C. Settembre, J.Z. Chen, P.R. Dormitzer, N. Grigorieff, S.C. Harrison, Atomic model of an infectious rotavirus particle, EMBO J. 30 (2011) 408–416.
[38] S. Amini-Bavil-Olyaee, Y.J. Choi, J.H. Lee, M. Shi, I.C. Huang, M. Farzan, J.U. Jung, The antiviral effector IFITM3 disrupts intracellular cholesterol homeostasis to block viral entry, Cell Host Microbe 13 (2013) 452–464.
[39] L.B. Tanner, B. Lee, The greasy response to virus infections, Cell Host Microbe 13 (2013) 375–377.
[40] M. Lakadamyali, M.J. Rust, X. Zhuang, Endocytosis of influenza viruses, Microbes Infect. 6 (2004) 929–936.
[41] S.N. Pattanakitsakul, J. Poungsawai, R. Kanlaya, S. Sinchaikul, S.T. Chen, V. Thongboonkerd, Association of Alix with late endosomal lysobisphosphatidic acid is important for dengue virus infection in human endothelial cells, J. Proteome Res. 9 (2010) 4640–4648.
[42] M. Lehto, V.M. Olkkonen, The OSBP-related proteins: a novel protein family involved in vesicle transport, cellular lipid metabolism, and cell signalling, Biochim. Biophys. Acta 2003 (1631) 1–11.
[43] W.A. Prinz, Non-vesicular sterol transport in cells, Prog. Lipid Res. 46 (2007) 297–314.
[44] M.H. Ngo, T.R. Colbourne, N.D. Ridgway, Functional implications of sterol transport by the oxysterol-binding protein gene family, Biochem. J. 429 (2010) 13–24.
[45] T.P. Levine, S. Munro, Targeting of Golgi-specific pleckstrin homology domains involves both PtdIns 4-kinase-dependent and -independent components, Curr. Biol. 12 (2002) 695–704.
[46] T.P. Levine, S. Munro, The pleckstrin homology domain of oxysterol-binding protein recognises a determinant specific to Golgi membranes, Curr. Biol. 8 (1998) 729–739.
[47] J.P. Wyles, C.R. McMaster, N.D. Ridgway, Vesicle-associated membrane protein-associated protein-A (VAP-A) interacts with the oxysterol-binding protein to modify export from the endoplasmic reticulum, J. Biol. Chem. 277 (2002) 29908–29918.
[48] C.J. Loewen, A. Roy, T.P. Levine, A conserved ER targeting motif in three families of lipid binding proteins and in Opi1p binds VAP, EMBO J. 22 (2003) 2025–2035.
[49] A. Goto, X. Liu, C.A. Robinson, N.D. Ridgway, Multisite phosphorylation of oxysterol-binding protein regulates sterol binding and activation of sphingomyelin synthesis, Mol. Biol. Cell 23 (2012) 3624–3635.
[50] C.J. Shoemaker, K.L. Schornberg, S.E. Delos, C. Scully, H. Pajouhesh, G.G. Olinger, L.M. Johansen, J.M. White, Multiple cationic amphiphiles induce a Niemann-Pick C phenotype and inhibit Ebola virus entry and infection, Plos One 8 (2013) e56265.
[51] M.K. Poh, G. Shui, X. Xie, P.Y. Shi, M.R. Wenk, F. Gu, U18666A, an intra-cellular cholesterol transport inhibitor, inhibits dengue virus entry and replication, Antivir. Res. 93 (2012) 191–198.
[52] T. Takano, K. Tsukiyama-Kohara, M. Hayashi, Y. Hirata, M. Satoh, Y. Tokunaga, C. Tateno, Y. Hayashi, T. Hishima, N. Funata, M. Sudoh, M. Kohara, Augmentation of DHCR24 expression by hepatitis C virus infection facilitates viral replication in hepatocytes, J. Hepatol. 55 (2011) 512–521.
[53] K. Sobo, I. Le Blanc, P.P. Luyet, M. Fivaz, C. Ferguson, R.G. Parton, J. Gruenberg, F.G. van der Goot, Late endosomal cholesterol accumulation leads to impaired intra-endosomal trafficking, PLoS One 2 (2007) e851.
[54] A. Civra, M.G. Giuffrida, M. Donalisio, L. Napolitano, Y. Takada, B.S. Coulson, A. Conti, D. Lembo, Identification of equine lactadherin-derived peptides that inhibit rotavirus infection via integrin receptor competition, J. Biol. Chem. 290 (2015) 12403–12414.
[55] M. Gutiérrez, P. Isa, C. Sánchez-San Martin, J. Pérez-Vargas, R. Espinosa, C.F. Arias, S. López, Different rotavirus strains enter MA104 cells through different endocytic pathways: the role of clathrin-mediated endocytosis, J. Virol. 84 (2010) 9161–9169.
[56] M. Soliman, J.Y. Seo, D.S. Kim, J.Y. Kim, J.G. Park, M.M. Alfajaro, Y.B. Baek, H.E. Cho, J. Kwon, J.S. Choi, M.I. Kang, S.I. Park, K.O. Cho, Activation of PI3K, Akt, and ERK during early rotavirus infection leads to V-ATPase-dependent endosomal acidification required for uncoating, PLoS Pathog. 14 (2018) e1006820.
[57] J.K. Livak, T.D. Schmittgen, Analysis of relative gene expression data using real-time quantitative PCR and the 2(-Delta Delta C(T)) method, Methods 25 (2001) 402–408.